Spectral properties of quasi-one-dimensional conductors with a finite transverse band dispersion

2008 J. Phys.: Condens. Matter 20 325239

(http://iopscience.iop.org/0953-8984/20/32/325239)

J. Phys.: Condens. Matter **20** (2008) 325239 (10pp) doi:10.1088/0953-8984/20/32/325239

Spectral properties of quasi-one-dimensional conductors with a finite transverse band dispersion

Ž Bonačić Lošić[1], A Bjeliš[2] and P Županović[1]

[1] Department of Physics, Faculty of Natural Sciences, Mathematics and Kinesiology, University of Split, Teslina 12, 21000 Split, Croatia
[2] Department of Physics, Faculty of Science, University of Zagreb, POB 162, 10001 Zagreb, Croatia

E-mail: agicz@pmfst.hr (Ž Bonačić Lošić) and bjelis@phy.hr

Received 2 June 2008, in final form 28 June 2008
Published 21 July 2008
Online at stacks.iop.org/JPhysCM/20/325239

Abstract

We determine the one-particle spectral function and the corresponding derived quantities for the conducting chain lattice with finite inter-chain hopping $t_\perp$ and three-dimensional long-range Coulomb electron–electron interaction. The standard G_0W_0 approximation is used. It is shown that, due to the optical character of the anisotropic plasmon dispersion caused by the finite $t_\perp$, a low energy quasi-particle δ-peak appears in the spectral function in addition to the hump present at energies of the order of the plasmon energy. Particular attention is devoted to the continuous crossover from the non-Fermi liquid regime to the Fermi liquid regime with increasing $t_\perp$. It is shown that the spectral weight of the hump transfers to the quasi-particle as the optical gap in the plasmon dispersion increases together with $t_\perp$, with the quasi-particle residuum Z behaving like $-(\ln t_\perp)^{-1}$ in the limit $t_\perp \to 0$. Our approach is appropriate for the wide range of energy scales given by the plasmon energy and the width of the conduction band, and is complementary to the Luttinger liquid techniques that are limited to the low energy regime close to the Fermi surface.

1. Introduction

Recent ARPES measurements of photoemission spectra show that a series of quasi-one-dimensional conductors, in particular the acceptor–donor chain compound TTF-TCNQ [1, 2] and Bechgaard salts $(TMTSF)_2X$ with X = PF_6, ClO_4, ReO_4, ... [3–5], have unusual properties, clearly distinguishable from those of the spectra of standard three-dimensional conductors. Quasi-particle peaks are absent for these compounds, and the spectra are instead dominated by a wide feature spread across energy scales of the order of the plasmon energies. Such data are in qualitative accordance with the conclusions of our recent calculation [6] for the spectral function of the one-dimensional electron band with three-dimensional long-range Coulomb electron–electron interaction, obtained within the so-called G_0W_0 approximation [7]. The physical origin of such behavior is the one-dimensionality of the electron band that causes an anisotropic acoustic plasmon dispersion. Since such dispersion spreads through the whole range of energies, from zero up to the plasmon energy Ω_{pl}, it introduces the wide feature into the spectral function at these energies, leaving thus no space for the creation of quasi-particle δ-peaks.

The spectral density $N(\omega)$ and other quantities related to the electron spectral properties have also been calculated exactly within the Luttinger liquid approach, using mostly the bosonization method [8, 9]. Such analyses are however limited to the narrow range of low energies $\omega \ll E_F, \Omega_{pl}$, where E_F is the Fermi energy of the order of bandwidth. It was shown that the spectral function shows, together with the absence of quasi-particle peaks, power-law behavior with the anomalous dimension α, defined by $N(\omega) \sim |\omega|^\alpha$ [8, 9] and interaction dependent. The comparison with measurements at low frequencies suggests values of anomalous dimension in the range $\alpha > 1$. This corresponds to the regime of strong three-dimensional long-range Coulomb interactions [10–14], which additionally suggests that the corresponding plasmon energy scale is not small, being at least of the order of the

bandwidth or larger. The G_0W_0 approximation is the only known approach which, as was already pointed out, enables the calculation of spectral properties over such wide ranges. However, it does not lead to the correct power-law exponent in the limit $\omega \to 0$. Hence, it is complementary to the Luttinger liquid approach [8, 9] which is concentrated on and limited to the low energy region.

The combination of the above two approaches thus covers the whole energy range relevant for the analysis of the photoemission properties of quasi-one-dimensional metals. As was already stated, the main emerging conclusion for the electron liquid with a strictly one-dimensional band dispersion is that, although three-dimensionally coupled through long-range Coulomb interaction, it does not show the essential property of Fermi liquids, namely the presence of quasi-particle excitations in the one-particle spectral properties. However in order to understand better the spectral properties of real quasi-one-dimensional conductors one has to take into account deviations from the one-dimensional band dispersion which come from finite inter-chain electron tunnelings. The corresponding question of both theoretical and experimental interest is that of how one re-establishes the Fermi liquid character of spectral properties by introducing and gradually increasing the transverse bandwidth $t_\perp$, approaching thus the regime of the standard isotropic three-dimensional conducting band.

In this work we address this question by extending our earlier G_0W_0 approach to the rectangular lattice of parallel chains with a finite transverse tunneling integral $t_\perp$. After taking into account the corresponding finite transverse curvature in the three-dimensional band dispersion [15, 16], the screened Coulomb interaction W_0 calculated within the random phase approximation (RPA) shows a finite optical plasmon gap proportional to $t_\perp$ in the long-wavelength limit. The plasmon dispersion thus has a three-dimensional, albeit strongly anisotropic, character for any finite value of $t_\perp$. A more detailed insight into the electron self-energy within the G_0W_0 approach shows that this property of plasmon dispersion has the dominant effect on the dressed electron propagator through the screened Coulomb interaction W_0, while the influence of finite $t_\perp$ through a bare electron propagator G_0 can be neglected. This enables an analytical derivation of the dressed electron Green's function and other quantities that follow from it.

The result obtained reveals the appearance of low energy quasi-particle peaks, in addition to the smeared structure at higher energies which is a characteristic of the strictly one-dimensional ($t_\perp = 0$) limit [6]. Note that the early G_0W_0 approach to the isotropic three-dimensional 'jellium' [17–19] led to an analogous result for the spectral function, showing quasi-particle peaks in the energy range $\mu - \Omega_{\rm pl} < \omega < \mu + \Omega_{\rm pl}$ where $\Omega_{\rm pl}$ is the minimum of the optical long-wavelength plasmon dispersion, and an additional structure due to the plasmon mode, with the finite spectral weight below and above these energies.

The spectral properties for the generalized Luttinger liquid with a weak electron tunneling between metallic chains and with the three-dimensional electron–electron Coulomb interaction were analyzed by using the appropriately developed higher dimensional bosonization technique [13, 14] in which the Fermi surface is approximated by a finite number of flat patches. This technique inherits in itself two approximations, namely the momentum transfer between different patches is ignored and the local band dispersion is linearized. On the other hand, it handles the case of $t_\perp \neq 0$ without having to rely on an expansion in powers of $t_\perp$ used in earlier studies of the model of parallel chains with a finite inter-chain hopping [20–24]. Using the four-patch approximation for the Fermi surface Kopietz *et al* [13, 14] obtained in the strong coupling limit the spectral function with the low energy quasi-particle having a weight proportional to $\Theta^{\gamma_{\rm cb}}$, $\Theta = |t_\perp|/E_{\rm F}$. Here $\gamma_{\rm cb}$ is the anomalous dimension of the corresponding Luttinger liquid for $t_\perp = 0$, and $E_{\rm F}$ is the Fermi energy. Furthermore, it is shown that there exists a large intermediate regime of wavevectors and frequencies where the Green's function satisfies the same anomalous scaling behavior as for $t_\perp = 0$. This is to be contrasted with the result of the perturbation treatment of $t_\perp$ [20] in which the quasi-particle peak appears only when the one-dimensional Green's function diverges, i.e. for the anomalous dimension less than unity.

Again, like in the case $t_\perp = 0$, the higher dimensional bosonization and our G_0W_0 approach are complementary, since the former is limited to the scaling behavior of the Green's function in the low energy range and the latter enables the reliable calculation of the wide maximum for the range of plasmon energy in the spectral function. It is important to note that the essential ingredient in both approaches is that the finite $t_\perp$ enters into calculations through the long-wavelength optical gap in the plasmon dispersion, and not through the corrugation of the band dispersion at the Fermi energy as in the perturbation approach of [20]. On the other hand, while both Wen's expansion in terms of $t_\perp$ [20] and the higher dimensional bosonization treatment cover low energy scaling, only the present G_0W_0 approach describes appropriately the crossover from the one-dimensional non-Fermi liquid regime to the three-dimensional Fermi liquid one for the whole range of energies.

In section 2 we calculate the electron Green's function within the G_0W_0 method developed in our previous work [6]. Section 3 is devoted to the spectral function. The density and the momentum distribution function are discussed in section 4. Section 5 contains concluding remarks.

2. Green's function

2.1. Dielectric function and excitations

We begin by considering the effect of finite transverse bandwidth on the plasmon dispersion. The electron band dispersion is modeled by

$$E(\mathbf{k}) = -2t_0(\cos k_\parallel b - \cos k_{\rm F} b) - 2t_\perp(\cos k_x a + \cos k_z c), \quad (1)$$

where b and a, c are longitudinal and two transverse lattice constants respectively, while t_0 and $t_\perp$ are corresponding

transfer integrals. The RPA polarization diagram now reads

$$\Pi(\mathbf{q},\omega)=\frac{4}{N_aN_bN_c}\times\sum_{k_x=-\frac{\pi}{a}}^{\frac{\pi}{a}}\sum_{k_\parallel=-\frac{\pi}{b}}^{\frac{\pi}{b}}\sum_{k_z=-\frac{\pi}{c}}^{\frac{\pi}{c}}\frac{n(\mathbf{k})[E(\mathbf{k}+\mathbf{q})-E(\mathbf{k})]}{(\omega+\mathrm{i}\eta\,\mathrm{sgn}\,\omega)^2-[E(\mathbf{k}+\mathbf{q})-E(\mathbf{k})]^2},\tag{2}$$

where

$$n(\mathbf{k})=\begin{cases}1, & E(\mathbf{k})<E_\mathrm{F}\\ 0, & E(\mathbf{k})>E_\mathrm{F}\end{cases}\tag{3}$$

is the occupation function. In the long-wavelength limit $\mathbf{q}\to 0$, where $\omega\gg E(\mathbf{k}+\mathbf{q})-E(\mathbf{k})$, the polarization diagram reduces to [25]

$$\Pi(\mathbf{q},\omega)=\frac{2}{N_aN_bN_c(\omega+\mathrm{i}\eta\,\mathrm{sgn}\,\omega)^2}\times\sum_{k_x=-\frac{\pi}{a}}^{\frac{\pi}{a}}\sum_{k_\parallel=-\frac{\pi}{b}}^{\frac{\pi}{b}}\sum_{k_z=-\frac{\pi}{c}}^{\frac{\pi}{c}}n(\mathbf{k})(\mathbf{q}\cdot\nabla_\mathbf{k})^2E(\mathbf{k})\tag{4}$$

with

$$(\mathbf{q}\cdot\nabla_\mathbf{k})^2E(\mathbf{k})=q_x^2\frac{\partial^2E(\mathbf{k})}{\partial k_x^2}+q_\parallel^2\frac{\partial^2E(\mathbf{k})}{\partial k_\parallel^2}+q_z^2\frac{\partial^2E(\mathbf{k})}{\partial k_z^2}.\tag{5}$$

Since by assumption $t_\perp\ll t_0$, the Fermi surface is only slightly corrugated, i.e. $\delta(k_x,k_z)/k_\mathrm{F}\ll 1$, where $\delta(k_x,k_z)$ is the deviation of the component of the Fermi wavevector in the chain direction from k_F, the latter being its value at $t_\perp=0$. The expansion of the band dispersion (1) in terms of δ up to the second order [15] leads to the equation for the Fermi surface

$$E(k_x,k_\mathrm{F}+\delta,k_z)\equiv v_\mathrm{F}\delta+E_\mathrm{F}''\delta^2/2-2t_\perp(\cos k_xa+\cos k_zc)=E_\mathrm{F}\tag{6}$$

where $v_\mathrm{F}=2t_0b\sin k_\mathrm{F}b$ is the Fermi velocity, $E_\mathrm{F}''\equiv\partial^2E(\mathbf{k})/\partial k_\parallel^2$ at $k_\parallel=k_\mathrm{F}$, and E_F is the shift of the Fermi energy with respect to its value for $t_\perp=0$. Our aim is to find out how $\delta(k_x,k_z)$ depends on $t_\perp$, and to determine the corresponding value of E_F. To this end we note that on switching to finite $t_\perp$ the band filling does not change, so

$$\int_{-\pi/a}^{\pi/a}\int_{-\pi/c}^{\pi/c}\delta(k_x,k_z)\,\mathrm{d}k_x\,\mathrm{d}k_z=0.\tag{7}$$

Then, since $\delta\sim t_\perp$ to the lowest order, the integration of equation (6) in terms of k_x and k_z gives $E_\mathrm{F}\sim t_\perp^2$. The explicit expansions follow after expressing $\delta(k_x,k_z)$ from equation (6),

$$\begin{aligned}\delta(k_x,k_z)&=-\frac{v_\mathrm{F}}{E_\mathrm{F}''}\times\left\{1\pm\sqrt{1-2\frac{E_\mathrm{F}''}{v_\mathrm{F}^2}[-E_\mathrm{F}-2t_\perp(\cos k_xa+\cos k_zc)]}\right\}\\&\approx\frac{2t_\perp}{v_\mathrm{F}}(\cos k_xa+\cos k_zc)+\frac{E_\mathrm{F}}{v_\mathrm{F}}-2\frac{E_\mathrm{F}''}{v_\mathrm{F}^3}t_\perp^2(\cos k_xa+\cos k_zc)^2.\end{aligned}\tag{8}$$

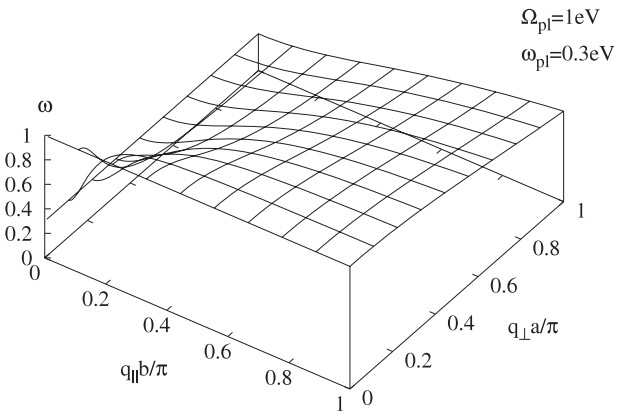

Figure 1. Plasmon dispersion $\omega(\mathbf{q})$ (see equation (15)).

Inserting this expression into the condition (7) one gets $E_\mathrm{F}=2E_\mathrm{F}''t_\perp^2/v_\mathrm{F}^2$, and finally

$$\delta(k_x,k_z)=\frac{2t_\perp}{v_\mathrm{F}}(\cos k_xa+\cos k_zc)+2\frac{E_\mathrm{F}''}{v_\mathrm{F}^3}t_\perp^2-2\frac{E_\mathrm{F}''}{v_\mathrm{F}^3}t_\perp^2(\cos k_xa+\cos k_zc)^2.\tag{9}$$

The expansion (9) enables the analytical derivation of the dielectric function $\varepsilon_m(\mathbf{q},\omega)=1-V(\mathbf{q})\Pi(\mathbf{q},\omega)$, where $V(\mathbf{q})=\frac{4\pi e^2}{v_0q^2}$ is the bare Coulomb interaction. After replacing

$$\sum_{k_x=-\frac{\pi}{a}}^{\frac{\pi}{a}}\sum_{k_\parallel=-\frac{\pi}{b}}^{\frac{\pi}{b}}\sum_{k_z=-\frac{\pi}{c}}^{\frac{\pi}{c}}n(\mathbf{k})\cdots\to\left(\frac{L}{2\pi}\right)^3\times\int_{-\frac{\pi}{a}}^{\frac{\pi}{a}}\mathrm{d}k_x\int_{-\frac{\pi}{c}}^{\frac{\pi}{c}}\mathrm{d}k_z\int_{-(k_\mathrm{F}+\delta)}^{k_\mathrm{F}+\delta}\mathrm{d}k_\parallel\cdots\tag{10}$$

in equation (4), and taking into account that

$$\int_{-(k_\mathrm{F}+\delta)}^{k_\mathrm{F}+\delta}\mathrm{d}k_\parallel\frac{\partial^2E(\mathbf{k})}{\partial k_\parallel^2}=2\frac{\partial E(\mathbf{k})}{\partial k_\parallel}\bigg|_0^{k_\mathrm{F}+\delta}=2(v_\mathrm{F}+E_\mathrm{F}''\delta+E_\mathrm{F}'''\delta^2/2)\tag{11}$$

and

$$\frac{\partial^2E(\mathbf{k})}{\partial k_x^2}=2t_\perp a^2\cos k_xa,\qquad\frac{\partial^2E(\mathbf{k})}{\partial k_z^2}=2t_\perp c^2\cos k_zc,\tag{12}$$

we get

$$\varepsilon_m(\mathbf{q},\omega)=1-\frac{\omega^2(\mathbf{q})}{(\omega+\mathrm{i}\eta\,\mathrm{sgn}\,\omega)^2}\tag{13}$$

with the plasmon dispersion given by

$$\omega^2(\mathbf{q})=\frac{\Omega_\mathrm{pl}^2q_\parallel^2+\omega_\mathrm{pa}^2q_x^2+\omega_\mathrm{pc}^2q_z^2}{q^2}.\tag{14}$$

Here longitudinal and transverse plasmon frequencies are given by $\Omega_\mathrm{pl}^2=\frac{8e^2v_\mathrm{F}}{ac}(1+2\frac{E_\mathrm{F}'''}{v_\mathrm{F}^2}t_\perp^2)$ and $\omega_\mathrm{pa}^2=\frac{16e^2t_\perp^2a}{cv_\mathrm{F}}$, $\omega_\mathrm{pc}^2=\frac{16e^2t_\perp^2c}{av_\mathrm{F}}$ respectively. Thus, the finiteness of the transverse bandwidth retains the optical character of the plasmon dispersion in all directions of the long-wavelength range $\mathbf{q}\to 0$, with the anisotropy scaled by the ratio $\frac{t_\perp}{t_0}$ as shown in figure 1. As long as $t_\perp\ll t_0$ we can skip the

correction proportional to $t_\perp^2$ in $\Omega_{\rm pl}^2$. Also, for simplicity we put $a = c$ and get the simplified expression for the long-wavelength plasmon dispersion,

$$\omega^2(\mathbf{q}) = \frac{\Omega_{\rm pl}^2 q_\parallel^2 + \omega_{\rm pl}^2 q_\perp^2}{q^2}, \tag{15}$$

with $\omega_{\rm pl}^2 = \frac{16e^2t_\perp^2}{v_{\rm F}}$ and $q_\perp^2 \equiv q_x^2 + q_z^2$. Note that in the regime of strong Coulomb interaction, $\Omega_{\rm pl} \gg t_0$ [6], we also have

$$\frac{\omega_{\rm pl}}{t_\perp} = \sqrt{\frac{ac}{2b^2}}\frac{\Omega_{\rm pl}}{t_0\sin(k_{\rm F}b)} \gg 1. \tag{16}$$

2.2. Green's function

In the calculation of the reciprocal Green's function $G^{-1}(\mathbf{k},\omega)$, we follow the G_0W_0 approximation [6]. The extension of this procedure obtained by the inclusion of the full $\mathbf{q}$ dependence in the band dispersion (1) leads to the generalization of the equation (20) in [6],

$$\begin{aligned} G^{-1}(\mathbf{k},\omega) &= \omega - E(\mathbf{k}) + {\rm i}\eta[1-2n(\mathbf{k})] - E_{\rm ex}(\mathbf{k}) \\ &\quad - \frac{1}{2N}\sum_{\mathbf{q}} V(\mathbf{q})\omega(\mathbf{q})\left[\frac{1-n(\mathbf{k}+\mathbf{q})}{\omega-\mu-\omega(\mathbf{q})-E(\mathbf{k}+\mathbf{q})+{\rm i}\eta}\right. \\ &\quad \left. + \frac{n(\mathbf{k}+\mathbf{q})}{\omega-\mu+\omega(\mathbf{q})-E(\mathbf{k}+\mathbf{q})-{\rm i}\eta}\right]. \end{aligned} \tag{17}$$

Here

$$E_{\rm ex}(\mathbf{k}) = -\frac{1}{N}\sum_{\mathbf{q}} V(\mathbf{q})n(\mathbf{k}+\mathbf{q}) \tag{18}$$

is the exchange energy per elementary cell for the one-particle state with the wavevector $\mathbf{k}$. Further simplification follows after noticing that, as long as we are in the regime of strong Coulomb interaction, $\Omega_{\rm pl} \gg t_0$ (see [6] and equation (16)), two second terms in the dispersion $E(\mathbf{k}+\mathbf{q}) \approx E_0(k_\parallel) + v_{\rm F}q_\parallel + E_\perp(k_a+q_a, k_{\rm c}+q_{\rm c})$ appearing in the denominators of equation (17) can be neglected with respect to that of the plasmon dispersion $\omega(\mathbf{q})$. As will be seen later, this approximation introduces small losses in the spectral density at low frequencies, but does not affect its main qualitative features. After a few nonessential simplifications which do not affect the physical content, like taking the flat Fermi surface at $|k_\parallel| = k_{\rm F}$ for the occupation function (3) and using cylindrical coordinates in the integration across the first Brillouin zone [6], one gets the analytical expression for $G^{-1}(\mathbf{k},\omega)$. Its real part reads

$$\begin{aligned} {\rm Re}\, G^{-1}(\mathbf{k},\omega) &= \omega - E(\mathbf{k}) + \frac{e^2}{2b}\left\{\ln\left[\left(\frac{bQ_\perp}{\pi}\right)^2+1\right]\right. \\ &\quad \left. + \frac{2bQ_\perp}{\pi}\arctan\frac{\pi}{bQ_\perp}\right\} - \frac{e^2}{2\pi}\left\{\frac{(\omega-\mu-E_0(k_\parallel))\omega_{\rm pl}}{(\omega-\mu-E_0(k_\parallel))^2-\omega_{\rm pl}^2}\right. \\ &\quad \times\frac{2\pi}{b}\left[\ln\frac{\omega_{\rm pl}}{\omega_{\rm pl}+\Omega_{\rm pl}} + \ln\left|\sqrt{1+\left(\frac{bQ_\perp}{\pi}\right)^2}\right.\right. \\ &\quad \left.\left. + \sqrt{\frac{\Omega_{\rm pl}^2}{\omega_{\rm pl}^2}+\left(\frac{bQ_\perp}{\pi}\right)^2}\right|\right] + \frac{(\omega-\mu-E_0(k_\parallel))^2}{(\omega-\mu-E_0(k_\parallel))^2-\omega_{\rm pl}^2} \\ &\quad \times\left[F\left(\frac{\pi}{b},\omega-\mu\right) - R(k_\parallel,\omega-\mu) + \frac{2\pi}{b}\right. \\ &\quad \left.\times\ln\left|\frac{(\omega-\mu-E_0(k_\parallel))\sqrt{1+\left(\frac{bQ_\perp}{\pi}\right)^2}-\omega_{\rm pl}\sqrt{\frac{\Omega_{\rm pl}^2}{\omega_{\rm pl}^2}+\left(\frac{bQ_\perp}{\pi}\right)^2}}{\omega-\mu-E_0(k_\parallel)-\Omega_{\rm pl}}\right|\right] \\ &\quad + Q_\perp\frac{(\omega-\mu-E_0(k_\parallel))\Omega_{\rm pl}^2}{\omega_{\rm pl}((\omega-\mu-E_0(k_\parallel))^2-\Omega_{\rm pl}^2)} \\ &\quad \times\int_{-\frac{\pi}{bQ_\perp}}^{\frac{\pi}{bQ_\perp}}\frac{{\rm d}y}{\sqrt{y^2+1}\sqrt{\frac{\Omega_{\rm pl}^2}{\omega_{\rm pl}^2}y^2+1}} \\ &\quad + Q_\perp\frac{(\omega-\mu-E_0(k_\parallel))^3(\omega_{\rm pl}^2-\Omega_{\rm pl}^2)}{\omega_{\rm pl}((\omega-\mu-E_0(k_\parallel))^2-\Omega_{\rm pl}^2)^2} \\ &\quad \left.\times\int_{-\frac{\pi}{bQ_\perp}}^{\frac{\pi}{bQ_\perp}}\frac{{\rm d}y}{\sqrt{y^2+1}\sqrt{\frac{\Omega_{\rm pl}^2}{\omega_{\rm pl}^2}y^2+1}\left[y^2+\frac{(\omega-\mu-E_0(k_\parallel))^2-\omega_{\rm pl}^2}{(\omega-\mu-E_0(k_\parallel))^2-\Omega_{\rm pl}^2}\right]}\right\} \end{aligned} \tag{19}$$

with functions R and F given by the expressions

$$\begin{aligned} R(k_\parallel,\omega) &= \left[R_1(k_{\rm F}-|k_\parallel|,\omega) + R_1(k_{\rm F}+|k_\parallel|,\omega)\right] \\ &\quad \times\Theta\left(\frac{\pi}{b}-|k_\parallel|-k_{\rm F}\right) + \left[R_1(k_{\rm F}-|k_\parallel|,\omega)\right. \\ &\quad \left. + 2R_1\left(\frac{\pi}{b},\omega\right) - R_1\left(\frac{2\pi}{b}-k_{\rm F}-|k_\parallel|,\omega\right)\right] \\ &\quad \times\Theta\left(k_{\rm F}+|k_\parallel|-\frac{\pi}{b}\right), \end{aligned} \tag{20}$$

with

$$R_1(x,\omega) = \begin{cases} -2x\ln|x| + x\ln\left|x^2+Q_\perp^2\dfrac{(\omega-E_0(k_\parallel))^2-\omega_{\rm pl}^2}{(\omega-E_0(k_\parallel))^2-\Omega_{\rm pl}^2}\right| \\ \quad + F(x,\omega), \qquad x\neq 0, \\ 0, \qquad x=0 \end{cases} \tag{21}$$

and

$$F(x,\omega) = \begin{cases} 2Q_\perp\sqrt{\dfrac{(\omega-E_0(k_\parallel))^2-\omega_{\rm pl}^2}{(\omega-E_0(k_\parallel))^2-\Omega_{\rm pl}^2}}\arctan\dfrac{x}{Q_\perp\sqrt{\frac{(\omega-E_0(k_\parallel))^2-\omega_{\rm pl}^2}{(\omega-E_0(k_\parallel))^2-\Omega_{\rm pl}^2}}} \\ \quad \text{for } |\omega-E_0(k_\parallel)|<\omega_{\rm pl}, \quad \Omega_{\rm pl}<|\omega-E_0(k_\parallel)|, \\ Q_\perp\sqrt{\dfrac{(\omega-E_0(k_\parallel))^2-\omega_{\rm pl}^2}{\Omega_{\rm pl}^2-(\omega-E_0(k_\parallel))^2}}\ln\left|\dfrac{x+Q_\perp\sqrt{\frac{(\omega-E_0(k_\parallel))^2-\omega_{\rm pl}^2}{\Omega_{\rm pl}^2-(\omega-E_0(k_\parallel))^2}}}{x-Q_\perp\sqrt{\frac{(\omega-E_0(k_\parallel))^2-\omega_{\rm pl}^2}{\Omega_{\rm pl}^2-(\omega-E_0(k_\parallel))^2}}}\right| \\ \quad \text{for } \omega_{\rm pl}<|\omega-E_0(k_\parallel)|<\Omega_{\rm pl}. \end{cases} \tag{22}$$

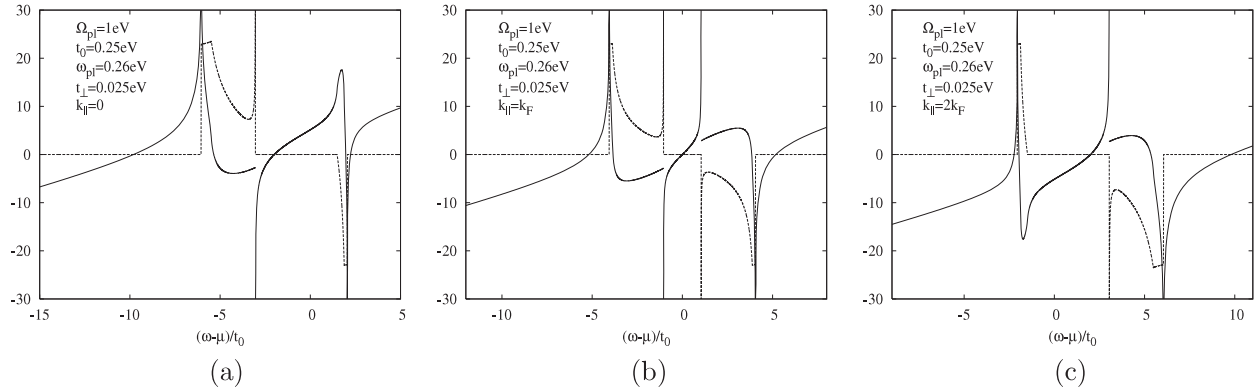

Figure 2. Frequency dependence of $\mathrm{Re}\,G^{-1}(k_\parallel,\omega)/t_0$ (full lines) and $-\mathrm{Im}\,G^{-1}(k_\parallel,\omega)/t_0$ (dashed lines) for $k_\mathrm{F}=\pi/2b$ and $k_\parallel=0$ (a), $k_\parallel=k_\mathrm{F}$ (b), and $k_\parallel=2k_\mathrm{F}$ (c).

The exchange energy in the expression (19) is given by

$$E_\mathrm{ex}(k_\parallel)=-\frac{e^2}{2\pi}\Bigg\{[H(k_\mathrm{F}-|k_\parallel|)+H(k_\mathrm{F}+|k_\parallel|)]\times\Theta\left(\frac{\pi}{b}-|k_\parallel|-k_\mathrm{F}\right)+\left[H(k_\mathrm{F}-|k_\parallel|)+2H\left(\frac{\pi}{b}\right)-H\left(\frac{2\pi}{b}-k_\mathrm{F}-|k_\parallel|\right)\right]\Theta\left(k_\mathrm{F}+|k_\parallel|-\frac{\pi}{b}\right)\Bigg\}\tag{23}$$

with

$$H(x)\equiv x\ln(Q_\perp^2+x^2)+2Q_\perp\arctan\frac{x}{Q_\perp}-x\ln x^2.\tag{24}$$

Further simplification follows upon realizing that in the regime of strong Coulomb interaction the self-energy contribution is dominant in comparison to the transverse dispersion term $2t_\perp(\cos k_x a+\cos k_z c)$ in $E(\mathbf{k})$. Consequently, we can skip the dependence of $\mathrm{Re}\,G^{-1}(\mathbf{k},\omega)$ on k_x and k_z as irrelevant for further considerations. Namely, after taking into account that $Q_\perp=2\sqrt{\pi}/\sqrt{ac}\ll\pi/b$, the leading contribution to the third term on the right-hand side in equation (19) reduces to $\frac{e^2}{2}Q_\perp\approx 0.16\frac{\omega_\mathrm{pl}\Omega_\mathrm{pl}}{t_\perp}\ll t_\perp$. This justifies the above approximation, after which we can proceed to a great extent along the lines of [6]. In particular, the chemical potential μ in equation (19) is now, after taking into account the self-consistent condition $\mathrm{Re}\,G^{-1}(k_\mathrm{F},\mu)=0$, given by

$$\mu=-\frac{e^2}{2b}\left\{\ln\left[\left(\frac{bQ_\perp}{\pi}\right)^2+1\right]+\frac{2bQ_\perp}{\pi}\arctan\frac{\pi}{bQ_\perp}\right\}.\tag{25}$$

The imaginary part of the reciprocal Green's function is given by

$$\mathrm{Im}\,G^{-1}(k_\parallel,\omega)=\frac{e^2}{2}\frac{(\omega-\mu-E_0(k_\parallel))^2}{(\omega-\mu-E_0(k_\parallel))^2-\omega_\mathrm{pl}^2}\times\Bigg\{2q_\mathrm{c}\Theta(\omega-\mu-E_0(k_\parallel))-[\Theta(-\omega+\mu+E_0(k_\parallel))+\Theta(\omega-\mu-E_0(k_\parallel))]\times\Bigg[2q_\mathrm{c}\Theta(k_\mathrm{F}-|k_\parallel|-q_\mathrm{c})+2k_\mathrm{F}\Theta(q_\mathrm{c}-|k_\parallel|-k_\mathrm{F})+(k_\mathrm{F}-|k_\parallel|+q_\mathrm{c})\times\Theta(|k_\parallel|+q_\mathrm{c}-k_\mathrm{F})\Theta(k_\mathrm{F}-||k_\parallel|-q_\mathrm{c}|)\times\Theta\left(\frac{2\pi}{b}-k_\mathrm{F}-|k_\parallel|-q_\mathrm{c}\right)+\left(2k_\mathrm{F}+2q_\mathrm{c}-\frac{2\pi}{b}\right)\times\Theta(k_\mathrm{F}-||k_\parallel|-q_\mathrm{c}|)\Theta\left(-\frac{2\pi}{b}+k_\mathrm{F}+|k_\parallel|+q_\mathrm{c}\right)\Bigg]\Bigg\}\tag{26}$$

for $\omega_\mathrm{pl}<|\omega-\mu-E_0(k_\parallel)|<\Omega_\mathrm{pl}$, and $\mathrm{Im}\,G^{-1}(k_\parallel,\omega)=0$ elsewhere. The wavenumber q_c in equation (26) is defined by

$$q_\mathrm{c}=\min\left(Q_\perp\sqrt{\frac{(\omega-\mu-E_0(k_\parallel))^2-\omega_\mathrm{pl}^2}{\Omega_\mathrm{pl}^2-(\omega-\mu-E_0(k_\parallel))^2}},\frac{\pi}{b}\right).\tag{27}$$

$\mathrm{Re}\,G^{-1}(k_\parallel,\omega)$ and $\mathrm{Im}\,G^{-1}(k_\parallel,\omega)$ are shown in figure 2 for three representative values of $k_\parallel$, namely for $k_\parallel$ equal to 0, k_F, and $2k_\mathrm{F}$. Let us at first look more closely into $\mathrm{Im}\,G^{-1}(k_\parallel,\omega)$. The vanishing of $\mathrm{Im}\,G^{-1}(k_\parallel,\omega)$ in the ranges $|\omega-\mu-E_0(k_\parallel)|<\omega_\mathrm{pl}$ and $|\omega-\mu-E_0(k_\parallel)|>\Omega_\mathrm{pl}$ can be traced already from the expression (17) after approximating $E(\mathbf{k}+\mathbf{q})\approx E_0(k_\parallel)$. Namely, in these ranges there are no poles of the reciprocal Green's function contributing to $\mathrm{Im}\,G^{-1}(k_\parallel,\omega)$.

$\mathrm{Im}\,G^{-1}(k_\parallel,\omega)$ vanishes also in the range $\mu+\omega_\mathrm{pl}+E_0(k_\parallel)<\omega<\mu+\omega(k_\parallel-k_\mathrm{F},Q_\perp)+E_0(k_\parallel)$ for $k_\parallel<k_\mathrm{F}$, as well as in the range $\mu-\omega(k_\parallel-k_\mathrm{F},Q_\perp)+E_0(k_\parallel)<\omega<\mu-\omega_\mathrm{pl}+E_0(k_\parallel)$ for $k_\parallel>k_\mathrm{F}$. This vanishing can also be traced from the expression (17). Namely, due to the presence of the occupation function $n(\mathbf{k}+\mathbf{q})$ in the $\mathbf{q}$-summation the non-vanishing contributions from dense discrete poles at $\omega=\mu-\omega(\mathbf{q})+E_0(k_\parallel)+\mathrm{i}\eta$ contribute only in the range $\mu-\Omega_\mathrm{pl}+E_0(k_\parallel)<\omega<\mu-\omega(k_\parallel-k_\mathrm{F},Q_\perp)+E_0(k_\parallel)$, while the non-vanishing contributions from poles at $\omega=\mu+\omega(\mathbf{q})+E_0(k_\parallel)-\mathrm{i}\eta$ contribute only in the range $\mu+\omega(k_\parallel-k_\mathrm{F},Q_\perp)+E_0(k_\parallel)<\omega<\mu+\Omega_\mathrm{pl}+E_0(k_\parallel)$.

In the range $\omega_\mathrm{pl}<|\omega-\mu-E_0(k_\parallel)|<\Omega_\mathrm{pl}$, $\mathrm{Im}\,G^{-1}(k_\parallel,\omega)$ is covered by the expression (26). It has a step singularity of the width $\frac{e^2k_\mathrm{F}\Omega_\mathrm{pl}^2}{\Omega_\mathrm{pl}^2-\omega_\mathrm{pl}^2}$ at $\omega=\mu\pm\Omega_\mathrm{pl}+E_0(k_\parallel)$ and diverges at the energies $\omega=\mu-\omega_\mathrm{pl}+E_0(k_\parallel)$ for $k_\parallel\leqslant k_\mathrm{F}$ and $\omega=\mu+\omega_\mathrm{pl}+E_0(k_\parallel)$ for $k_\parallel\geqslant k_\mathrm{F}$. At energies $\omega_{1,2}=\mu\mp\omega(\pi/b,Q_\perp)+E_0(k_\parallel)$, $\mathrm{Im}\,G^{-1}(k_\parallel,\omega)$ has the respective anomalous minimum and maximum, with jumps in the first derivatives. These

extrema originate from the confinement of the **q**-summation in the expression (17) to the first Brillouin zone. The integration in terms of $q_\perp$ from 0 to $Q_\perp$ results in the limitation on the $q_\parallel$-integration to the range $|q_\parallel| < Q_\perp\sqrt{\frac{(\omega-\mu-E_0(k_\parallel))^2-\omega_{\rm pl}^2}{\Omega_{\rm pl}^2-(\omega-\mu-E_0(k_\parallel))^2}}$ as long as this limit is within the first Brillouin zone. However, for values of ω in the ranges $\mu-\Omega_{\rm pl}+E_0(k_\parallel) < \omega < \mu-\omega(\pi/b, Q_\perp)+E_0(k_\parallel)$ and $\mu+\omega(\pi/b, Q_\perp)+E_0(k_\parallel) < \omega < \mu+\Omega_{\rm pl}+E_0(k_\parallel)$ we have $\frac{\pi}{b} < Q_\perp\sqrt{\frac{(\omega-\mu-E_0(k_\parallel))^2-\omega_{\rm pl}^2}{\Omega_{\rm pl}^2-(\omega-\mu-E_0(k_\parallel))^2}}$, so the $q_\parallel$-integration is limited to the first Brillouin zone, i.e. by the ω-independent boundary $q_{\rm c}=\frac{\pi}{b}$. The resulting values of $\mathrm{Im}\,G^{-1}(k_\parallel,\omega)$ at the anomalous minimum and maximum are $\mp e^2 k_{\rm F}\frac{(\omega_{1,2}-\mu-E_0(k_\parallel))^2}{(\omega_{1,2}-\mu-E_0(k_\parallel))^2-\omega_{\rm pl}^2}$.

Let us now consider $\mathrm{Re}\,G^{-1}(k_\parallel,\omega)$. As is seen from figure 2, it diverges towards $\pm\infty$ at the respective energies $\omega=\mu\mp\Omega_{\rm pl}+E_0(k_\parallel)$ at which $\mathrm{Im}\,G^{-1}(k_\parallel,\omega)$ has step singularities. These singularities are shifted towards larger values of ω as $k_\parallel$ increases. The zeros of $\mathrm{Re}\,G^{-1}(k_\parallel,\omega)$ at $\omega<\mu-\Omega_{\rm pl}+E_0(k_\parallel)$ and $\omega>\mu+\Omega_{\rm pl}+E_0(k_\parallel)$ are also shifted to the right as $k_\parallel$ increases, the former approaching the singularity at $\omega=\mu-\Omega_{\rm pl}+E_0(k_\parallel)$ and the latter increasing the distance from the singularity at $\omega=\mu+\Omega_{\rm pl}+E_0(k_\parallel)$. $\mathrm{Re}\,G^{-1}(k_\parallel,\omega)$ also has essential singularities at $\omega=\mu-\omega_{\rm pl}+E_0(k_\parallel)$ (for $k_\parallel\leqslant k_{\rm F}$) and $\omega=\mu+\omega_{\rm pl}+E_0(k_\parallel)$ (for $k_\parallel\geqslant k_{\rm F}$), i.e. at energies at which $\mathrm{Im}\,G^{-1}(k_\parallel,\omega)$ diverges.

The zero of $\mathrm{Re}\,G^{-1}(k_\parallel,\omega)$ in the range $\mu-\omega_{\rm pl}+E_0(k_\parallel) < \omega < \mu+\omega_{\rm pl}+E_0(k_\parallel)$ in which $\mathrm{Im}\,G^{-1}(k_\parallel,\omega)$ vanishes is the low energy pole of the electron propagator $G(k_\parallel,\omega)$. It is of the form $y(k_\parallel)=\widetilde{E}(k_\parallel)-\mathrm{i}\Gamma(k_\parallel)$, where $\Gamma(k_\parallel)$ is infinitesimally small in the present approach. Accordingly, our Green's function has in this range the standard resonant form

$$G(k_\parallel,\omega)=\frac{Z(k_\parallel)}{\omega-y(k_\parallel)}, \tag{28}$$

where $Z(k_\parallel)=|\partial\,\mathrm{Re}\,G^{-1}(k_\parallel,y(k_\parallel))/\partial\omega|^{-1}$ is the residuum of the Green function at the pole $y(k_\parallel)$. We emphasize that the low energy pole appears due to the optical gap $\omega_{\rm pl}$ in the long-wavelength plasmon dispersion introduced by the finite inter-chain transfer integral $t_\perp$ in the electron dispersion. This is illustrated by the analytical expression for the residuum $Z(k_\parallel)$ at $k_\parallel=k_{\rm F}$ in the limit $\omega_{\rm pl}\ll\Omega_{\rm pl}$,

$$Z_{\rm F}=1\Big/\left[1+\frac{e^2}{\pi}\frac{Q_\perp}{\Omega_{\rm pl}}\ln\left(\frac{4\Omega_{\rm pl}}{\omega_{\rm pl}}\right)\right]$$
$$=1\Big/\left[1+\frac{e^2}{\pi}\frac{Q_\perp}{\Omega_{\rm pl}}\ln\left(\frac{\Omega_{\rm pl}\sqrt{v_{\rm F}}}{et_\perp}\right)\right]. \tag{29}$$

The dependences of $Z_{\rm F}$ on $t_\perp$ obtained numerically as well as with the use of the expression (29) are shown in figure 3. The Green's function has the standard resonant form (28) also in the frequency range $|\omega-\mu-E_0(k_\parallel)| > \Omega_{\rm pl}$ in which $\mathrm{Re}\,G^{-1}(k_\parallel,\omega)$ has zeros and $\mathrm{Im}\,G^{-1}(k_\parallel,\omega)$ vanishes.

On the other hand the structure of the Green's function in the region $\omega_{\rm pl} < |\omega-\mu-E_0(k_\parallel)| < \Omega_{\rm pl}$ in which $\mathrm{Im}\,G^{-1}(k_\parallel,\omega)\neq 0$ is influenced by the plasmon dispersion contribution to the expression (17).

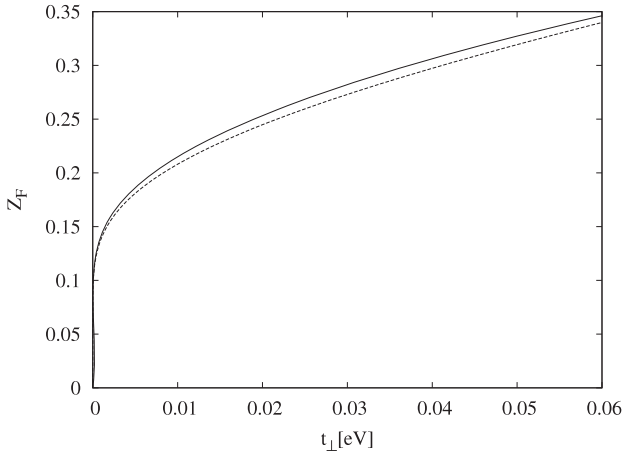

Figure 3. $Z_{\rm F}$ obtained numerically (full curve) and from the expression (29) (dashed curve).

3. Spectral function

The single-particle spectral function is defined by

$$A(k_\parallel,\omega)=\frac{1}{\pi}|\mathrm{Im}\,G(k_\parallel,\omega)|. \tag{30}$$

It can be directly expressed in terms of $\mathrm{Re}\,G^{-1}(k_\parallel,\omega)$ and $\mathrm{Im}\,G^{-1}(k_\parallel,\omega)$,

$$A(k_\parallel,\omega)=\frac{1}{\pi}\frac{|\mathrm{Im}\,G^{-1}(k_\parallel,\omega)|}{[\mathrm{Re}\,G^{-1}(k_\parallel,\omega)]^2+[\mathrm{Im}\,G^{-1}(k_\parallel,\omega)]^2}, \tag{31}$$

except for the case of $\mathrm{Re}\,G^{-1}(k_\parallel,\omega)$ having a zero $y(k_\parallel)$ in the frequency range in which $\mathrm{Im}\,G^{-1}(k_\parallel,\omega)=0$, when it is represented by the quasi-particle δ-peak

$$A(k_\parallel,\omega)=Z(k_\parallel)\delta(\omega-y(k_\parallel)). \tag{32}$$

The spectral function $A(k_\parallel,\omega)$, obtained after inserting expressions (19) and (26) into equations (31) and (32), is shown in figure 4 for two values of the transverse plasmon frequency, $\omega_{\rm pl}=0.26$ and 0.63 eV. Generally it is characterized by the coexistence of wide humps and quasi-particle δ-peaks. Humps originate from the plasmon dispersion in the range $\omega_{\rm pl} < |\omega-\mu-E_0(k_\parallel)| < \Omega_{\rm pl}$. Their positions vary slowly with the wavenumber $k_\parallel$. As for the δ-peaks, they are situated in the energy ranges $\mu+E_0(k_\parallel)-\omega_{\rm pl} < \omega < \mu+E_0(k_\parallel)+\omega_{\rm pl}$ and $|\omega-\mu-E_0(k_\parallel)| > \Omega_{\rm pl}$. It is to be noted that δ-peaks are present for any finite $t_\perp$. However, the decrease of $t_\perp$ leads to the decrease of the weight of the quasi-particle δ-peak in the range $\mu+E_0(k_\parallel)-\omega_{\rm pl} < \omega < \mu+E_0(k_\parallel)+\omega_{\rm pl}$ in favor of the growing weight of the hump. In the limit $t_\perp\to 0$, i.e. $\omega_{\rm pl}\to 0$, these quasi-particles disappear and all their spectral weight transfers to the hump. The vanishing of the quasi-particle weight in the range $\mu+E_0(k_\parallel)-\omega_{\rm pl} < \omega < \mu+E_0(k_\parallel)+\omega_{\rm pl}$ as $t_\perp\to 0$ is visible in the dependence of $Z(k_\parallel)$ on $t_\perp$ for $k_\parallel=k_{\rm F}$ as shown by equation (29) and in figure 3. We thus come to the spectral function for $t_\perp=0$ which has no low energy quasi-particle. In other words, the crossover from the $t_\perp\neq 0$ Fermi liquid regime to the $t_\perp=0$

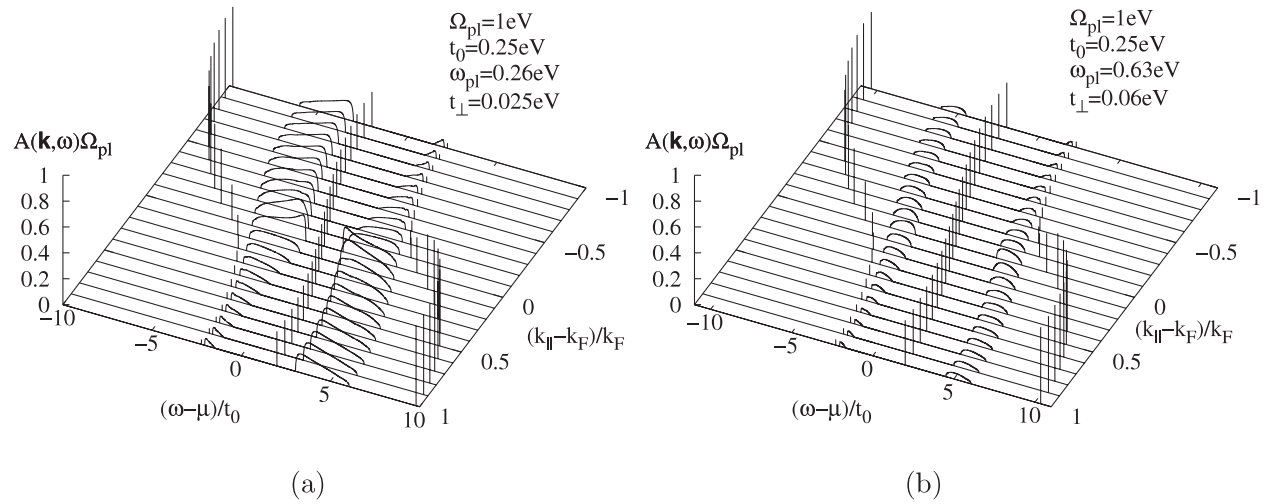

Figure 4. Spectral function $A(k_\parallel, \omega)$ for small ($\omega_{\rm pl} = 0.26$ eV) (a) and large ($\omega_{\rm pl} = 0.63$ eV) (b) values of the transverse plasmon frequency $\omega_{\rm pl}$ in the case $k_{\rm F} = \pi/2b$. Broad maxima for different values of the wavenumber $k_\parallel$ follow from equation (31), while δ-peaks are represented by their weight $Z(k_\parallel)$ according to equation (32).

non-Fermi liquid regime takes place through the decrease of the quasi-particle weight by closing the optical gap in the long-wavelength plasmon mode.

We note that the numerically obtained spectral function shown in figure 4 fulfills excellently the sum rule

$$\int_{-\infty}^{\infty} A(k_\parallel, \omega)\, {\rm d}\omega = 1, \tag{33}$$

with the agreement up to 10^{-4} over the whole range of the wavevector $k_\parallel$, and for all values of $t_\perp$ considered. Finally, we notice that, in contrast to the quasi-particles in the range $\mu + E_0(k_\parallel) - \omega_{\rm pl} < \omega < \mu + E_0(k_\parallel) + \omega_{\rm pl}$, the quasi-particles in the energy range $|\omega - \mu - E_0(k_\parallel)| > \Omega_{\rm pl}$ are not critically sensitive to the plasmon optical gap $\omega_{\rm pl}$ and keep a finite intensity in the limit $t_\perp \to 0$ as was already shown in [6].

As was already mentioned in the introduction, the main property of the above spectral function, namely the quasi-particles at low energies coexisting with the wide structure originating from the collective plasmon branch, resembles the result obtained in the early investigation of the isotropic 'jellium' model within the G_0W_0 approach by Hedin and Lundqvist [17–19]. They showed that due to the finite long-wavelength minimum in the optical plasmon dispersion, $\Omega_{\rm pl}$, a quasi-particle with reduced weight appears in the region $\mu - \Omega_{\rm pl} < \omega < \mu + \Omega_{\rm pl}$, while the rest of the spectral weight is widely distributed at energies outside this range.

As was already argued in [6], the non-Fermi liquid regime for $t_\perp = 0$ is in the qualitative agreement with the ARPES spectra of Bechgaard salts which apparently do not show low energy quasi-particles [3–5]. On the other hand, the present results for the spectral function of the quasi-one-dimensional metal in the $t_\perp \neq 0$ Fermi liquid regime suggest that in $(TMTSF)_2PF_6$ (for which $t_\perp = 0.0125$ eV and $t_0 = 0.125$ eV) the quasi-particle δ-peak with the weight of the order of 20% of the total spectral weight for a given value of $k_\parallel$ is expected in the low energy range, at an energy distance of the order of $\omega_{\rm pl} = 0.13$ eV from the lower edge of the wide hump. A more directed experimental search, supported by improved energy and intensity resolutions, is very probably necessary for finding peaks with such weak intensities.

Finally, we refer to the work [26] devoted to the quasi-two-dimensional metals with the finite transverse transfer integral $t_\perp$ between metallic planes, with the main result analogous to ours. Namely the spectral function in this case also consists of the suppressed quasi-particle peak and a broad feature. Again, the RPA screened Coulomb interaction gives a strongly anisotropic plasmon branch dispersion of the form (15) containing a small transverse plasmon frequency compared with the longitudinal one. This result is in agreement with the ARPES spectra of quasi-two-dimensional high-$T_{\rm c}$ superconductors in the normal conducting phase [27].

4. The density of states and momentum distribution function

Integrating numerically the spectral density $A(k_\parallel, \omega)$ in terms of $k_\parallel$, we get the density of states for band electrons,

$$n(\omega) = \frac{1}{2k_{\rm F}} \int_0^{\frac{\pi}{b}} A(k_\parallel, \omega)\, {\rm d}k_\parallel, \tag{34}$$

shown in figure 5 for two values of the inter-chain transfer integral, $t_\perp = 0.025$ and 0.06 eV. Three distinctive step singularities in $n(\omega)$ originate from the edges of the corresponding quasi-particle δ-peak dispersions. In particular, the density of states falls from a maximum at the lowest energy of the $k_\parallel$ dependent quasi-particle δ-peak in the range $\omega < \mu + E_0(k_\parallel) - \Omega_{\rm pl}$ to a local minimum. Then it rises until the step discontinuity at the highest energy of the quasi-particle δ-peak in the energy range $\omega < \mu + E_0(k_\parallel) - \Omega_{\rm pl}$ is reached. Further on, $n(\omega)$ varies slowly from this discontinuity until the next one at the lowest energy of the quasi-particle δ-peak in the energy range $\mu + E_0(k_\parallel) - \omega_{\rm pl} < \omega < \mu + E_0(k_\parallel) + \omega_{\rm pl}$ is reached, accumulating the contribution from the spectral

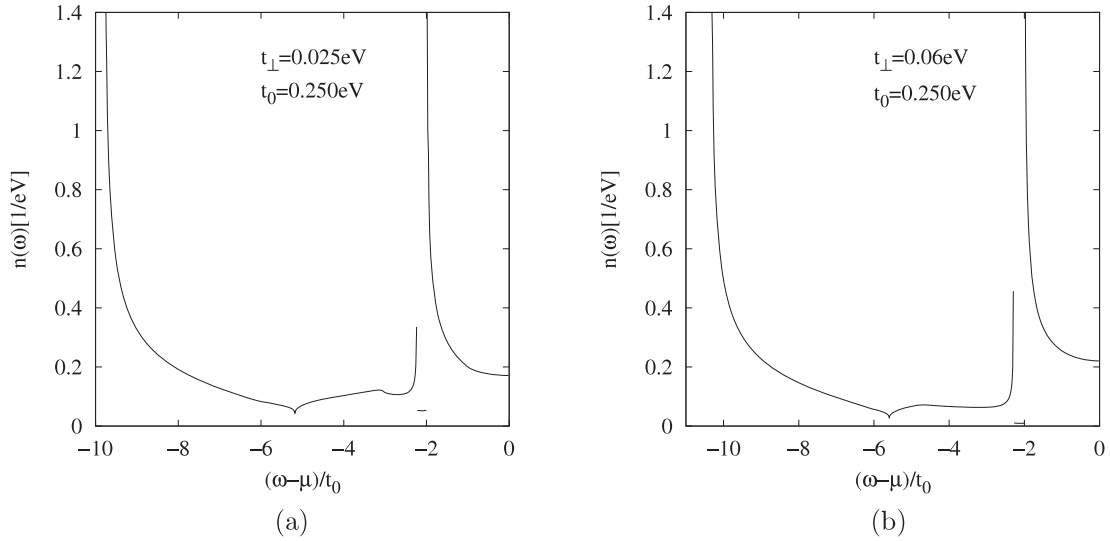

Figure 5. Density of states $n(\omega)$ for $t_\perp$ equal 0.025 eV (a) and 0.06 eV (b).

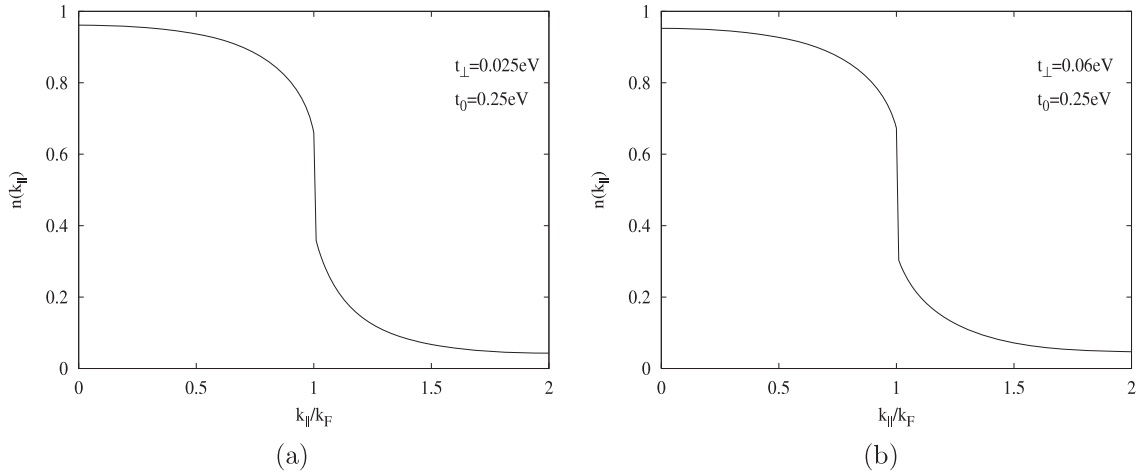

Figure 6. Momentum distribution function for $k_F = \frac{\pi}{2b}$ and $t_\perp$ equal 0.025 eV (a) and 0.06 eV (b) showing the discontinuity at k_F.

density hump in this range. Increasing further the energy above the third step discontinuity, one comes to the minimum of $n(\omega)$ at $\omega = \mu$, the latter bearing the contribution from the quasi-particle at the chemical potential in the spectral function.

The momentum distribution function

$$n(k_\parallel) = \int_{-\infty}^{\mu} A(k_\parallel, \omega)\, \mathrm{d}\omega \tag{35}$$

is also calculated numerically, and shown in figure 6 for $t_\perp = 0.025$ eV (a) and 0.06 eV (b). The deviation of areas below the curves (a) and (b) from the exact number of particles is smaller than 0.1%, indicating the highly satisfactory self-consistency of the G_0W_0 approximation. The momentum distribution has the qualitative behavior of the dressed Fermi liquid. It decreases from the maximal value at $k_\parallel = 0$ towards the step discontinuity at the Fermi wavenumber $k_\parallel = k_F$. The height of this discontinuity is equal to the spectral weight $Z(k_F)$ of the quasi-particle δ-peak at $\omega = \mu$. Figure 6 again shows that this height decreases as $t_\perp$ decreases.

5. Conclusion

The aim of the present analysis is twofold.

Firstly, we investigate the crossover from the specific spectral function of the one-dimensional conducting band to that of standard isotropic three-dimensional Fermi liquid. We show that the absence of quasi-particle peaks is limited to the band with the strictly one-dimensional flat Fermi surface. Quasi-particle peaks appear immediately upon introducing a finite corrugation of the Fermi surface, measured by finite $t_\perp$ in our approach. The spectral weight of these δ-peaks for $k_\parallel = k_F$ is given by the expression (29) and shown in figure 3. It has a non-power-law dependence on the transverse bandwidth [$Z \sim -(\ln t_\perp)^{-1}$] in the limit $t_\perp \to 0$. The rest of the spectral weight is carried by the wide feature in the energy range characterized by the plasmon energy Ω_{pl}. As is shown in section 2, this result is to a great extent obtained analytically after a few technical simplifications which are well justified in the limit $t_\perp \ll t_0, \Omega_{pl}$.

Although, due to this limitation, our method of calculation cannot be extended towards the pure three-dimensional regime ($t_\perp \approx t_0$), the plausible expectation is that the quasi-particle spectral weight will increase continuously as $t_\perp$ further increases, approaching the three-dimensional regime with quantitative properties obtained a long time ago by Hedin and Lundquist [17–19]. It is worthwhile to stress again that, as the above Z versus $t_\perp$ dependence illustrates, the present calculations, unlike some others (e.g. [20, 21]), are not simple power-law expansions in terms of $t_\perp$, and in this respect are complementary to the higher dimensional bosonization approach developed in [13, 14]. The essential reason for the inadequacy of the perturbation approach in terms of $t_\perp$, even in the limit $t_\perp \to 0$, is to be recognized in a qualitative change of the plasmon spectrum, namely in the opening of the gap in its long-wavelength limit. This gap in turn enables the appearance of quasi-particles in $A(\mathbf{k}, \omega)$ already within the G_0W_0 approximation. A word of warning here concerns the applicability of the G_0W_0 approximation itself. Strictly, it is limited to the range of weakly screened Coulomb interaction, the relevant criterion being $\Omega_{\rm pl} < t_0$. In some of illustrations presented here we allow values of $\Omega_{\rm pl}$ above this range, anticipating that no qualitatively new situation arises in the intermediate range $\Omega_{\rm pl} \approx t_0$. This range, as well as the range of strong long-range Coulomb interaction (even after the RPA screening is taken into account), however, still awaits a better understanding.

The present analysis can also provide some estimations on the possible observability of simultaneous appearance of quasi-particles and wide humps in experiments measuring spectral properties. The energy resolution in reported photoemission measurements on Bechgaard salts varied between 10 and 30 meV [3–5]. Additional complication comes from indications that surface effects could have affected low energy parts of existing ARPES data [28]. Thus in order to observe a dispersing sharp low energy quasi-particle with the narrow width ranging up to 10 meV, it will be necessary to have an increased energy resolution at low energies and an enhanced bulk sensitivity of the ARPES spectra. We believe that such demands are achievable, particularly because our estimations suggest that the spectral weights of quasi-particle peaks are expected to range up to 20% of the total spectral weight, and to be positioned at binding energies ranging up to energies of the order of 250 meV, appearing in coexistence with characteristic wide humps already observed at higher energies.

Among quasi-one-dimensional materials investigated in photoemission measurements the acceptor–donor chain compound TTF-TCNQ appears to be a particularly interesting example [1, 2]. There are various indications, e.g. the infrared optical measurements [29–31], that it has a soft longitudinal mode at 10 meV in the metallic phase. This mode was explained theoretically within the model of the quasi-one-dimensional metal with two bands per donor and acceptor chains and the three-dimensional RPA screened electron–electron interaction [32]. It was shown that the appearance of such a mode in the low energy range is due to the strong coupling between the plasmon and the collective inter-band dipolar mode. As for the ARPES spectra, they show the absence of low energy quasi-particles and the one-dimensional dispersion of electron bands [1, 2]. However the bandwidth values from these data are two to four times larger than the values obtained by earlier theoretical and experimental estimations [33]. This signals that it is necessary to include electron–electron interactions in order to improve quantitative interpretation of the data. More precisely, it remains to investigate the influence of the elsewhere observed low energy mode on the low energy spectral properties of the quasi-one-dimensional metal with one electron band per donor and acceptor chains within the G_0W_0 approximation, but with the RPA screened Coulomb electron–electron interaction obtained for the model with two bands per chain [32]. Taking into account the results that we obtained in [6] and in the present work, we expect this low energy mode to also be responsible for the low energy spectral properties of TTF-TCNQ. The full analysis of this question is under way.

Acknowledgment

The work was supported by project 119-1191458-1023 of the Croatian Ministry of Science, Education and Sports.

References

[1] Zwick F *et al* 1998 *Phys. Rev. Lett.* **81** 2974
[2] Claessen R *et al* 2002 *Phys. Rev. Lett.* **88** 096402
[3] Zwick F *et al* 1997 *Phys. Rev. Lett.* **79** 3982
[4] Zwick F *et al* 2000 *Solid State Commun.* **113** 179
[5] Zwick F *et al* 2000 *Eur. Phys. J.* B **13** 503
[6] Bonačić Lošić Ž, Županović P and Bjeliš A 2006 *J. Phys.: Condens. Matter* **18** 3655
[7] Hedin L 1965 *Phys. Rev.* **139** A796
[8] Meden V and Schönhammer K 1992 *Phys. Rev.* B **46** 15753
[9] Voit J 1993 *J. Phys.: Condens. Matter* **5** 8305
[10] Barišić S 1983 *J. Physique* **44** 185
[11] Schulz H J 1983 *J. Phys. C: Solid State Phys.* **16** 6769
[12] Botrić S and Barišić S 1984 *J. Physique* **45** 185
[13] Kopietz P, Meden V and Schönhammer K 1995 *Phys. Rev. Lett.* **74** 2999
[14] Kopietz P, Meden V and Schönhammer K 1997 *Phys. Rev.* B **56** 7232
[15] Kwak J F 1982 *Phys. Rev.* B **26** 4789
[16] Agić Ž, Županović P and Bjeliš A 2004 *J. Physique* IV **114** 95
[17] Hedin L and Lundqvist S 1969 *Solid State Physics* vol 23, ed F Seitz and D Turnbull (New York: Academic) p 1
[18] Lundqvist B I 1967 *Phys. Kondens. Mater.* **6** 206
[19] Lundqvist B I 1968 *Phys. Kondens. Mater.* **7** 117
[20] Wen X G 1990 *Phys. Rev.* B **42** 6623
[21] Bourbonnais C and Caron L G 1991 *Int. J. Mod. Phys.* B **5** 1033
[22] Boies D, Bourbonnais C and Tremblay A-M S 1995 *Phys. Rev. Lett.* **74** 968
[23] Clarke D G and Strong S P 1996 *J. Phys.: Condens. Matter* **8** 10089
[24] Tsvelik A M 1996 *Preprint* cond-mat/9607209
[25] Ziman J M 1972 *Principles of the Theory of Solids* (Cambridge: Cambridge University Press)
[26] Artemenko S N and Remizov S V 2001 *JETP Lett.* **74** 430 (*Preprint* cond-mat/0109264)
[27] Dessau D S *et al* 1993 *Phys. Rev. Lett.* **71** 2781

[28] Sing M *et al* 2003 *Phys. Rev.* B **67** 125402
[29] Tanner D B *et al* 1976 *Phys. Rev.* B **13** 3381
[30] Jacobsen C S 1979 *Lecture Notes in Physics* vol 95, ed S Barišić *et al* (Berlin: Springer) p 223
[31] Basista H *et al* 1990 *Phys. Rev.* B **42** 4088
[32] Županović P, Bjeliš A and Barišić S 1999 *Europhys. Lett.* **45** 188
[33] Jérome D and Schulz H J 1982 *Adv. Phys.* **31** 299